Journal of Sound and Vibration 326 (2009) 383–399

Contents lists available at ScienceDirect

Journal of Sound and Vibration

journal homepage: www.elsevier.com/locate/jsvi

Control of a piezoelectric actuator considering hysteresis

Oriol Gomis-Bellmunt [a,*], Fayçal Ikhouane [b], Daniel Montesinos-Miracle [a]

[a] CITCEA-DEE-UPC Center of Technological Innovation in Static Converters and Drives, Electrical Engineering Department, Universitat Politècnica de Catalunya, Av. Diagonal 647 08028, Barcelona, Spain

[b] Departament de Matemàtica Aplicada III, Escola Universitària d'Enginyeria Tècnica Industrial de Barcelona, Universitat Politècnica de Catalunya, Comte d'Urgell, 187, 08036 Barcelona, Spain

ARTICLE INFO

Article history:
Received 21 October 2008
Received in revised form
31 March 2009
Accepted 1 May 2009
Handling Editor: J. Lam
Available online 10 June 2009

ABSTRACT

This paper deals with the modeling and control of a piezoelectric actuator. The main challenge for the control design is the presence of hysteresis. This nonlinearity is represented in this paper using the Bouc–Wen model and a time-varying PID controller is designed for micropositioning purpose. The performance of the controller is tested using numerical simulations and experimentally.

1. Introduction

Although the so-called classical actuators (electromagnetic, hydraulic and pneumatic) are the most used in the industry, new technologies based on different physical principles are being developed. In applications where the size of the actuator has to be minimized, or where fast response and high resolution are needed, the classical actuators fail to respond appropriately. For this reason, non-classical technologies are becoming more relevant. Among them, the piezoelectric actuators [1–3] are proving to be a reliable solution for many engineering applications, ranging from micropositioning (machine tools, optic devices or modern microscopes) to active control of structures.

The piezoelectric actuators are based on the known piezoelectric effect described in 1880 by Jacques and Pierre Curie [4]: in certain materials with crystalline non-symmetrical structure, dipoles are formed when the material is deformed, i.e. a mechanical strain produces an electrical field; reciprocally, the application of an electric field produces a strain. These actuators show a fast reaction time, a high resolution, a high energy density and an easy miniaturization. However, the piezoelectric actuators have some drawbacks: the reduced strain ($<0.2\%$), the presence of nonlinearities and the high voltage needed for optimal performance. In this paper, we focus on the nonlinear behavior of piezoelectric actuators by taking into account the presence of hysteresis. In materials, the hysteresis is referred to the memory nature of inelastic systems where the restoring force depends not only on the instantaneous deformation but also on the history of that deformation.

To describe the behavior of hysteretic processes several mathematical models have been proposed [5]: the Duhem model [6] uses the property that a hysteretic system's output changes its character when the input changes direction; the Ishlinskii hysteresis operator has been proposed as a model for plasticity–elasticity [7]; the Preisach model has been used for the modeling of electromagnetic hysteresis [8]; the Bouc–Wen model has been used to model wood joints and structural systems [9]. A survey of the mathematical models for hysteresis may be found in [10]. These models have been

* Corresponding author. Tel.: +34 934016727; fax: +34 934017433.
E-mail address: oriol.gomis@upc.edu (O. Gomis-Bellmunt).
URLS: http://www.citcea.upc.edu (O. Gomis-Bellmunt), http://www-ma3.upc.es/codalab (F. Ikhouane).

0022-460X/$ - see front matter © 2009 Elsevier Ltd. All rights reserved.
doi:10.1016/j.jsv.2009.05.011

applied to describe the behavior of piezoelectric actuators: Prandtl–Ishlinskii in [11], Preisach in [12–15] and Bouc–Wen in [16]. An energy based model has been employed in [17]. The Maxwell resistive-capacitor model has been used in a number of studies [18–21] to model piezoceramic hysteresis for position and vibration control applications.

In this work we represent a piezoelectric actuator by the Bouc–Wen model for smooth hysteresis [22]. This model consists in a first-order nonlinear state equation, and an output equation where the input and state signals appear linearly. This model has received an increasing interest due to its ability to capture in an analytical form a range of shapes of hysteretic cycles which match the behavior of a wide class of hysteretical systems [23]. In particular, it has been used to model piezoelectric elements [16], magnetorheological dampers [24,25] and wood joints [9]. The models, derived from experiments, have been used either to predict the behavior of the physical hysteretic element [24] or for control purposes as in [26–29].

In this paper we consider the problem of micropositioning using a piezoelectric actuator. This problem has spurred much interest in the current literature. A robust controller is employed in [26] to control a piezoelectric bimorph actuator using the Bouc–Wen model. In [30] a piezoelectric actuator is modeled with neural networks and controlled with a variable structure control system. In [31], the controller uses information of the charge instead of the voltage for the control of position. This technique takes advantage of the reduced hysteresis between the displacement and the electrical charge, but presents some difficulty for the measurement of the charge. Since the piezoelectric device is represented in this work using the Bouc–Wen model, the results of [28] are used and improved for the control of the piezoelectric element. In [28], a second-order mechanical system that includes a Bouc–Wen hysteresis is considered for control purposes. The control objective is to guarantee the global boundedness of all the closed loop signals, and the regulation of both the displacement and the velocity of the device to zero. This objective is achieved using a simple PID controller. However, the main drawback of this controller is that the equilibrium point of the closed loop system is not robust vis-à-vis perturbations which is undesirable in practice. The main contributions of this paper are the following:

- We present a new control law which is a time-varying PID that guarantees that the equilibrium point of the closed loop is robust to perturbations.
- This control law is tested in numerical simulations and experimentally using a piezoelectricactuator.

The main advantage of the proposed control law over other existing control schemes is that it is simple to implement in an industrial context.

2. Background results

2.1. PID control of a Bouc–Wen hysteresis

We consider the second-order mechanical system described by

$$m\ddot{x}(t) + c\dot{x}(t) + \Phi(x)(t) = u(t) \tag{1}$$

with initial conditions $x(0)$, $\dot{x}(0)$ and excited by a control input force $u(t)$. The output restoring force Φ is assumed to be described by the normalized Bouc–Wen model [32]:

$$\Phi(x)(t) = \kappa_x x(t) + \kappa_w w(t) \tag{2}$$

$$\dot{w}(t) = \rho(\dot{x}(t) - \sigma|\dot{x}(t)|\,|w(t)|^{n-1}w(t) + (\sigma - 1)\dot{x}(t)|w(t)|^n) \tag{3}$$

with an initial condition $w(0)$. The parameters $n \geq 1$, $\rho > 0$, $\sigma \geq \frac{1}{2}$, $\kappa_x > 0$, $\kappa_w > 0$, $m > 0$ and $c \geq 0$ are unknown. The range of the parameters corresponds to the Class I Bouc–Wen model which is stable, asymptotically dissipative and thermodynamically consistent [32]. The displacement $x(t)$ and velocity $\dot{x}(t)$ are available through measurements, but the signal $w(t)$ is not. Let $y_r(t)$ be a (known) smooth and bounded reference signal whose (known) smooth and bounded derivatives are such that $\lim_{t\to\infty} y_r(t) = \lim_{t\to\infty} \dot{y}_r(t) = \lim_{t\to\infty} \ddot{y}_r(t) = \lim_{t\to\infty} y_r^{(3)}(t) = 0$ exponentially. This means that there exist some constants $a > 0$ and $b > 0$ such that $|y_r^{(i)}(t)| \leq ae^{-bt}$ for $t \geq 0$ and $i = 0, 1, 2, 3$.

The control objective is to globally asymptotically regulate the displacement $x(t)$ and velocity $\dot{x}(t)$ to the reference signals $y_r(t)$ and $\dot{y}_r(t)$preserving the global boundedness of all the closed loop signals; that is $x(t)$, $\dot{x}(t)$, $w(t)$ and $u(t)$.

We assume the following:

Assumption 1. The unknown parameters lie in known intervals. That is we have $m \in [m_{\min}, m_{\max}]$ with $m_{\min} > 0$, $c \in [0, c_{\max}]$, $\kappa_x \in (0, \kappa_{x_{\max}}]$, $\kappa_w \in (0, \kappa_{w_{\max}}]$, $\sigma \in [\frac{1}{2}, \sigma_{\max}]$, $\rho \in (0, \rho_{\max}]$.

Note that the unknown structure parameter $n \geq 1$ is not required to lie in a known interval.

The problem of controlling the system (1)–(3) has been treated in [28], where it is demonstrated that a PID control insures that the displacement and velocity errors tend to zero. Introduce the variables:

$$x_1(t) = x(t) - y_r(t), \quad x_2(t) = \dot{x}(t) - \dot{y}_r(t), \quad x_0(t) = \int_0^t x_1(\tau)\,\mathrm{d}\tau \tag{4}$$

and choose as a control law the PID controller:

$$u(t) = -k_0 x_0(t) - k_1 x_1(t) - k_2 x_2(t) \tag{5}$$

where the k_i's are design parameters. Then we have [28]

Theorem 1. *Consider the closed loop formed by system* (1)–(3) *and the control law* (5). *Define the following constants*:

$$k_{2_{\min}} = \sqrt{[]}2m_{\max}(\sigma_{\max}\rho_{\max}\kappa_{w_{\max}} + \kappa_{x_{\max}} + k_1) \tag{6}$$

$$e_1 = \frac{(c_{\max} + k_2)^3}{m_{\min}^2}$$

$$e_2 = \frac{k_1^2}{m_{\max}^2}(k_2^2 - k_{2_{\min}}^2)$$

$$k_{0_{\max}} = \min\left(\frac{k_1 k_2}{m_{\max}}, -e_1 + \sqrt{[]}e_1^2 + e_2\right) \tag{7}$$

and choose the design gains k_0, k_1 *and* k_2 *in the following way*: *take any positive value for* k_1; *then choose* k_2 *such that* $k_2 > k_{2_{\min}}$; *finally take* $0 < k_0 < k_{0_{\max}}$. *In this case we have the following*:

(1) *All the closed loop signals* x_0, x_1, x_2, w *and the control* u *are globally bounded.*
(2) $\lim_{t\to\infty} x(t) = 0$ *and* $\lim_{t\to\infty} \dot{x}(t) = 0$.

2.2. Forced limit cycle description of a Bouc–Wen hysteresis

In this section, we consider the system composed only of the two equations (2) and (3) where the input is $x(t)$ and the output is $\Phi(x)(t)$. We consider in this section that the displacement signal is periodic so that the output $\Phi(x)(t)$ is also asymptotically periodic [32]. The objective of this section is to characterize analytically the asymptotic limit cycle.

2.2.1. Class of inputs

In this section, we consider that the input signal $x(t)$ is wave T-periodic [32]. This means that it is continuous on the time interval $[0, +\infty)$ and periodic of period $T > 0$. Furthermore there exists a scalar $0 < T^+ < T$ such that the signal x is C^1 on both intervals $(0, T^+)$ and (T^+, T) with $\dot{x}(\tau) = \mathrm{d}x(\tau)/\mathrm{d}\tau > 0$ for $\tau \in (0, T^+)$ and $\dot{x}(\tau) < 0$ for $\tau \in (T^+, T)$. We denote $X_{\min} = x(0)$ and $X_{\max} = x(T^+) > X_{\min}$ the minimal and maximal values of the input signal, respectively (see Fig. 1). Periodic sine and triangular signals are also wave periodic.

2.2.2. Analytic description

The Bouc–Wen limit cycle is described using the following functions that are useful for solving analytically the differential equation (3):

$$\varphi_{\sigma,n}^{-}(\mu) = \int_0^{\mu} \frac{\mathrm{d}u}{1 + \sigma|u|^{n-1}u + (\sigma - 1)|u|^n} \tag{8}$$

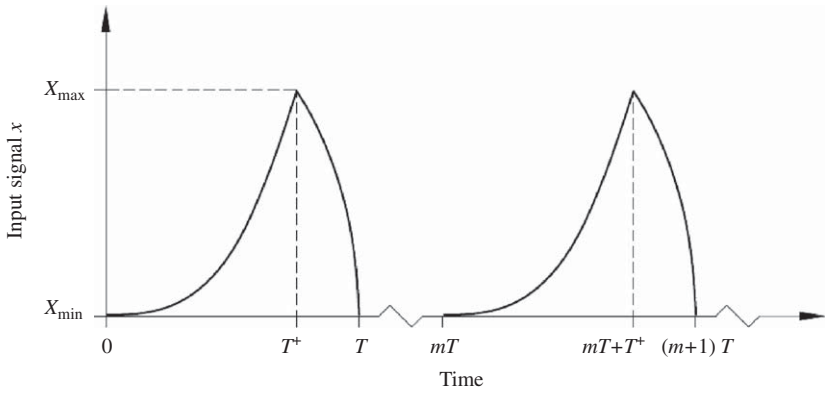

Fig. 1. Example of a T-wave periodic signal.

$$\varphi^{+}_{\sigma,n}(\mu) = \int_0^{\mu} \frac{\mathrm{d}u}{1-\sigma|u|^{n-1}u+(\sigma-1)|u|^n} \tag{9}$$

$$\varphi_{\sigma,n}(\mu) = \varphi^{+}_{\sigma,n}(\mu) + \varphi^{-}_{\sigma,n}(\mu) \tag{10}$$

for any scalar $\mu \in (-1,1)$. It has been shown in [32] that the functions $\varphi^{-}_{\sigma,n}(\cdot)$, $\varphi^{+}_{\sigma,n}(\cdot)$ and $\varphi_{\sigma,n}(\cdot)$ are strictly increasing on the interval $(-1,1)$ so that they are bijective. Their inverses are denoted by $\psi^{-}_{\sigma,n}(\cdot)$, $\psi^{+}_{\sigma,n}(\cdot)$ and $\psi_{\sigma,n}(\cdot)$, respectively. The limit cycle for the Bouc–Wen model is described by the following [32]:

Theorem 2. *Let $x(t)$ be a wave T-periodic input signal. Define the functions ω_m and F_m for any positive integer m as follows*:

$$\omega_m(\tau) = w(mT+\tau) \quad \textit{for } \tau \in [0,T] \tag{11}$$

$$\phi_m(\tau) = \kappa_x x(\tau) + \kappa_w \omega_m(\tau) \quad \textit{for } \tau \in [0,T] \tag{12}$$

Then the sequence of functions $\{\phi_m\}_{m\geq 1}$ (resp. $\{\omega_m\}_{m\geq 1}$) converges uniformly on the interval $[0,T]$ to a continuous function $\bar{\Phi}$ (resp. $\bar{w}$) defined as

$$\bar{\Phi}(\tau) = \kappa_x x(\tau) + \kappa_w \bar{w}(\tau) \quad \textit{for } \tau \in [0,T] \tag{13}$$

$$\bar{w}(\tau) = \psi^{+}_{\sigma,n}(\varphi^{+}_{\sigma,n}[-\psi_{\sigma,n}(\rho(X_{\max}-X_{\min}))] + \rho(x(\tau)-X_{\min})) \quad \textit{for } \tau \in [0,T^{+}] \tag{14}$$

$$\bar{w}(\tau) = -\psi^{+}_{\sigma,n}(\varphi^{+}_{\sigma,n}[-\psi_{\sigma,n}(\rho(X_{\max}-X_{\min}))] - \rho(x(\tau)-X_{\max})) \quad \textit{for } \tau \in [T^{+},T] \tag{15}$$

Furthermore we have for all $\tau \in [0,T]$

$$-1 < -\psi_{\sigma,n}(\rho(X_{\max}-X_{\min})) \leq \bar{w}(\tau) \leq \psi_{\sigma,n}(\rho(X_{\max}-X_{\min})) < 1$$

the lower and upper bounds of $\bar{w}(\tau)$ being attained at $\tau = 0$ and $\tau = T^{+}$, respectively.

This result means that the output restoring force goes asymptotically to a periodic function. The transient behavior is captured by Eqs. (11) and (12) while the steady-state is captured by Eqs. (13)–(15). The loading part of the limit cycle is described by Eqs. (13) and (14), while the unloading part is described by Eqs. (13) and (15). Loosely speaking, the functions $\bar{\Phi}$ and $\bar{w}$ denote the steady-state responses of the functions Φ and w, respectively.

3. Experimental platform

3.1. Experimental layout

The system under study is the patch of Fig. 2 which is a piezoelectric actuator that contains the foil PIC-255 (Physik Instrumente). The piezoelectric actuator uses the d_{31} mode and it is seen as a SISO system whose input is the voltage u applied to the 3 axis and the output is the displacement y along the 1 axis.

The actuator can be used in a number of applications ranging from active control of structures to micropositioning and optics applications. For the sake of completeness, we give the physical characteristics of the patch. The piezoelectric ceramic used is a PI (Physik Instrumente) PIC-255. The material shows a d_{31} piezoelectric coefficient of $-180\times10^{-12}\,\mathrm{m\,V^{-1}}$, dielectric permittivity $\varepsilon^{T}_{33}/\varepsilon_0$ of 1800, elastic constant s^{E}_{11} of $16.1\times10^{-12}\,\mathrm{m^2\,N^{-1}}$, density of $7.80\,\mathrm{g\,cm^{-3}}$ and Curie temperature of 350 °C. The piezoelectric foil shows a weight of 2.34 g and dimensions of 50 mm × 30 mm × 0.2 mm and the entire patch a weight of 3.405 g and dimensions of 60 mm × 35 mm × 0.5 mm. The piezoelectric actuator lays in a low friction surface where it is clamped in one extreme and left free in the other in order to allow its free movement.

The experiments have been undertaken with the platform sketched in Fig. 3. The control is performed by a *DSP*[1] controller. The actuator is driven by means of a power amplifier whose working voltage is set by the *DSP* controller. The amplifiercan work with voltages between −450 and 450 V with a maximum current of 100 mA.

The displacement of the free edge of the piezoelectric actuator is measured using a laser triangulator *Micro-Epsilon optoNCDT 1607* with range 500 μm, bandwidth 10 kHz and resolution 0.1 μm. The data have been acquired with a four channel *Yokogawa DL9000* (bandwidth 500 MHz). All the quantities have been sampled so that at least 25 000 samples are provided for each plot.

3.2. System modeling

The system model is given by [26]

$$m'\ddot{x}(t) + c'\dot{x}(t) + \kappa_a x(t) = \kappa_b \Phi(u)(t) \tag{16}$$

[1] DSP stands for digital signal processor.

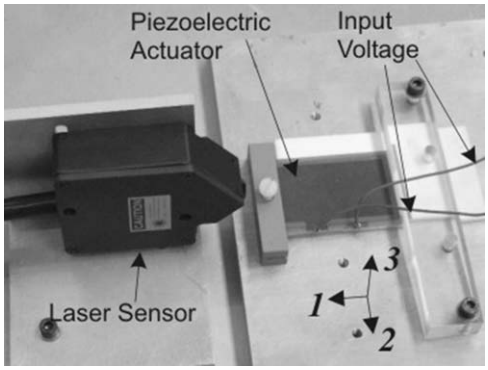

Fig. 2. Controlled piezoelectric actuator.

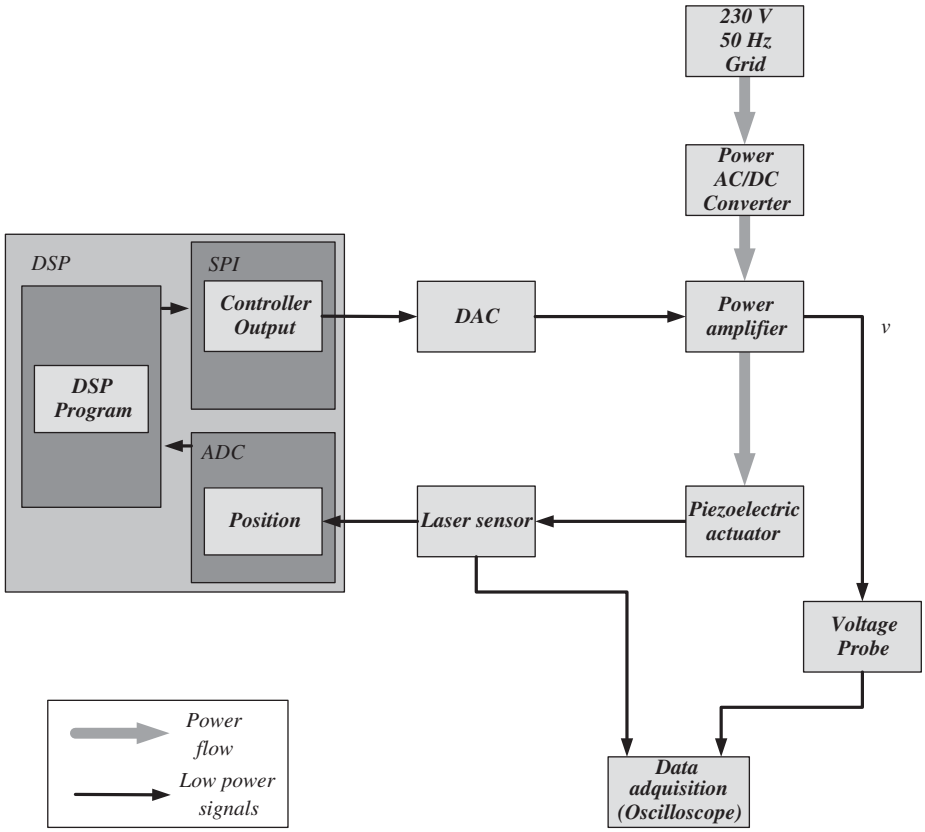

Fig. 3. Block diagram of the platform.

where κ_a and κ_b are elastic constants, m' and c' are the equivalent mass and damping coefficient of the piezoelectric actuator, $x(t)$ its relative position with respect to the sensor, and $k_b\Phi(u)(t)$ is the force produced by the actuator. The term $\Phi(u)(t)$ is assumed to follow a Bouc–Wen equation so that the actuator may be represented by

$$m'\ddot{y}(t) + c'\dot{y}(t) + \kappa_a(y(t) - y_0) = \kappa_b\kappa'_x u(t) + \kappa_b\kappa'_w w(t) \tag{17}$$

$$\dot{w}(t) = \rho(\dot{y}(t) - \sigma|\dot{y}(t)|\,|w(t)|^{n-1}w(t) + (\sigma - 1)\dot{y}(t)|w(t)|^n) \tag{18}$$

where κ'_w and κ'_x are constant gains. The nonlinear term $w(t)$ takes into account the effect of hysteresis.

Defining

$$m = \frac{m'}{\kappa_a\kappa'_x}, \quad c = \frac{c'}{\kappa_a\kappa'_x}, \quad \kappa_x = \frac{\kappa_a}{\kappa_b k'_x}, \quad \kappa_w = -\frac{\kappa'_w}{\kappa'_x} \tag{19}$$

it can be seen that the actuator follows Eqs. (1)–(3). This model is valid only for low frequencies (well below the resonance of the actuator), as an important mismatch has been observed experimentally for high frequencies.

3.3. Control objective

The control objective is to insure the boundedness of all the closed loop signals, along with the regulation of the displacement and velocity of the piezoelectric actuator to zero. Furthermore, in steady-state, the control output has to have a unique value so that the closed loop system has a unique equilibrium point.

4. Parameter identification

The system under consideration is described by Eqs. (1)–(3) in which the system parameters m, c along with the Bouc–Wen model parameters κ_x, κ_w, ρ, σ, n are unknown. The objective of this section is to determine these parameters using the measurements of the relative displacement $x(t)$ and the voltage input $u(t)$. Since we are dealing with a model valid only for low frequencies, the terms $m\ddot{x}$ and $c\dot{x}$ can be neglected in Eq. (1) so that the actuator model can be approximated by Eqs. (2) and (3).

The problem of identifying the parameters of the Bouc–Wen model (2)–(3) has been treated in Ref. [33]. The technique presented in this reference consists in choosing for $u(t)$ a periodic signal with a loading–unloading shape (that is a wave periodic signal [32]). This implies that $x(t)$ is also wave periodic so that a limit cycle (x, u) is obtained asymptotically. The experimentally obtained limit cycle is then used to determine the unknown Bouc–Wen model parameters.

The identified parameters are given in Fig. 4. It can be seen that these parameters are almost constant in the frequency range $[0, 100\,\text{Hz}]$. The parameter values are shown in Table 1.

For higher values of the frequency, the Bouc–Wen model parameters are highly frequency dependent.

Model (2)–(3) is tuned with the parameters obtained in Table 1 (column 4), and the initial condition is calculated fromEq. (2) as

$$w(0) = \frac{u(0) - k_x x(0)}{k_w} \tag{20}$$

To check the validity of this model, it is excited with a random signal whose frequency content lies in the interval $[0, 100\,\text{Hz}]$. Fig. 5 gives the responses of both the model and the actuator. A reasonable match is observed.

5. Control laws

This section introduces three control laws for the piezoelectric device, which are based on the linear controller of Section 2. These controllers are tested by means of numerical simulations.

5.1. PID control

In this section we consider the closed loop formed by system (1)–(3) along with the control law (5). The closed loop is then described by the equations:

$$\dot{x}_0 = x_1 \tag{21}$$

$$\dot{x}_1 = x_2 \tag{22}$$

$$\dot{x}_2 = m^{-1}(-(c + k_2)x_2 - (\kappa_x + k_1)x_1 - k_0 x_0 - \kappa_w w - m\ddot{y}_r - c\dot{y}_r - \kappa_x y_r) \tag{23}$$

$$\dot{w} = \rho(x_2 + \dot{y}_r - \sigma|x_2 + \dot{y}_r|\,|w|^{n-1}w + (\sigma - 1)(x_2 + \dot{y}_r)|w|^n) \tag{24}$$

where w is time dependent. In order to determine the PID constants k_0, k_1 and k_2, we need to have known bounds on the unknown parameters (Assumption 1). The identification process of Section 4 gives these bounds for the Bouc–Wen model parameters κ_x, κ_w, ρ, σ, n. Section 3.1 gives information on the rest of the system parameters. We use the following bounds:

- $m_{\min} = 3.98 \times 10^{-3}\,\text{V s}^2\,\text{m}^{-1}$
- $m_{\max} = 6.63 \times 10^{-3}\,\text{V s}^2\,\text{m}^{-1}$
- $c_{\max} = 13.43\,\text{V s m}^{-1}$
- $k_{x\max} = 10.8 \times 10^{6}\,\text{V m}^{-1}$
- $\sigma_{\max} = 0.9212$
- $\rho_{\max} = 9.510 \times 10^{4}\,\text{m}^{-1}$
- $k_{w\max} = 48.74\,\text{V}$

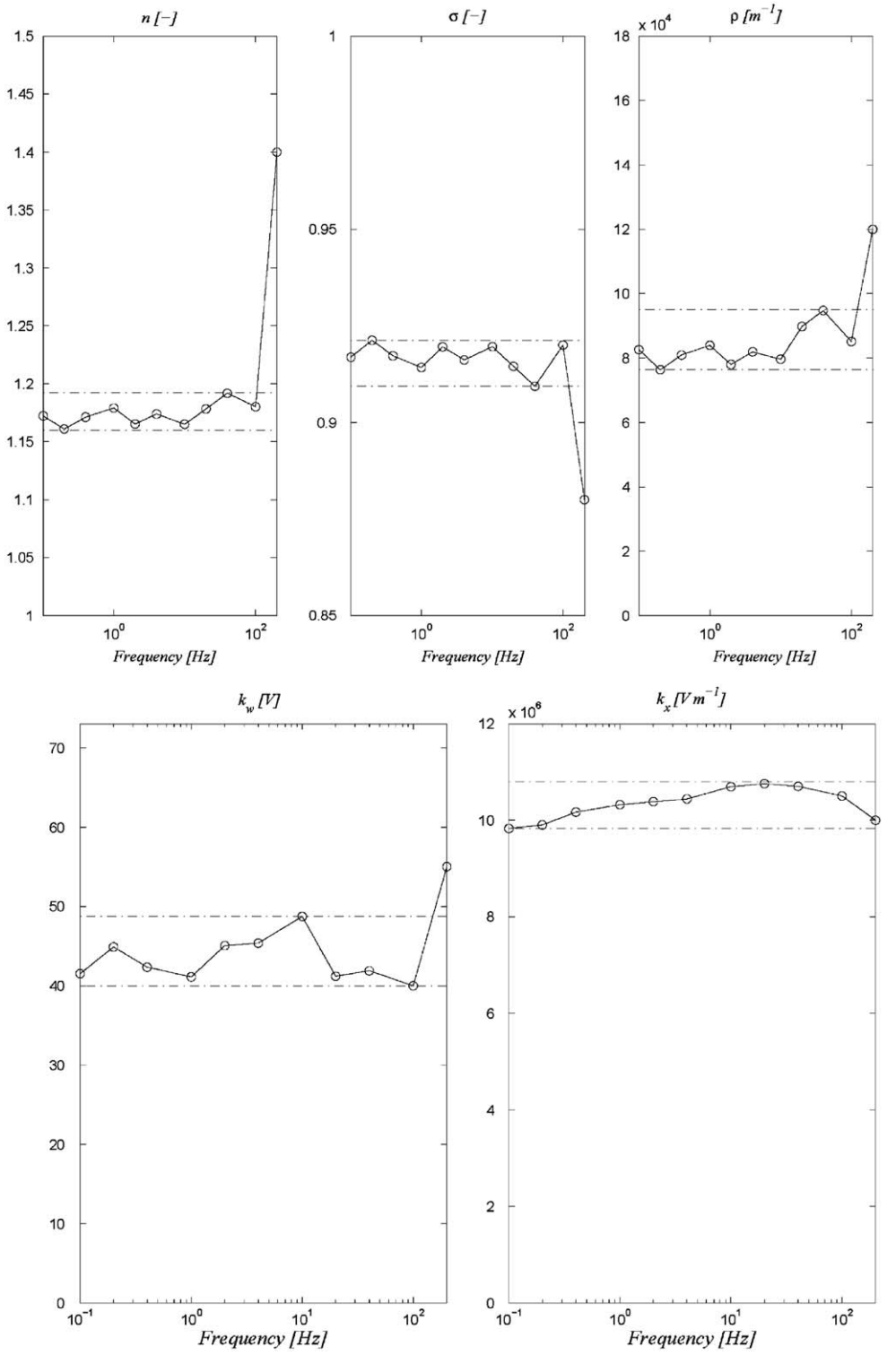

Fig. 4. Identified parameters for different input frequencies.

The PID controller parameters are determined using Theorem 1. The first design parameter to be chosen is $k_1 = 5 \times 10^6$ so that we get $k_{2\,\min} = 567.6$. We choose $k_2 = 580$ so that we obtain $k_{0\,\max} = 1.16 \times 10^9$. Finally we take $k_0 = 1 \times 10^9$.

Table 1
Identified parameters.

Parameter	Smallest value	Largest value	Mean value	Unit
n	1.16	1.192	1.176	–
σ	0.9094	0.9212	0.9153	–
ρ	7.632×10^4	9.5×10^4	8.566×10^4	m^{-1}
k_w	39.97	48.74	43.57	V
k_x	9.83×10^6	10.8×10^6	10.35×10^6	$V\,m^{-1}$

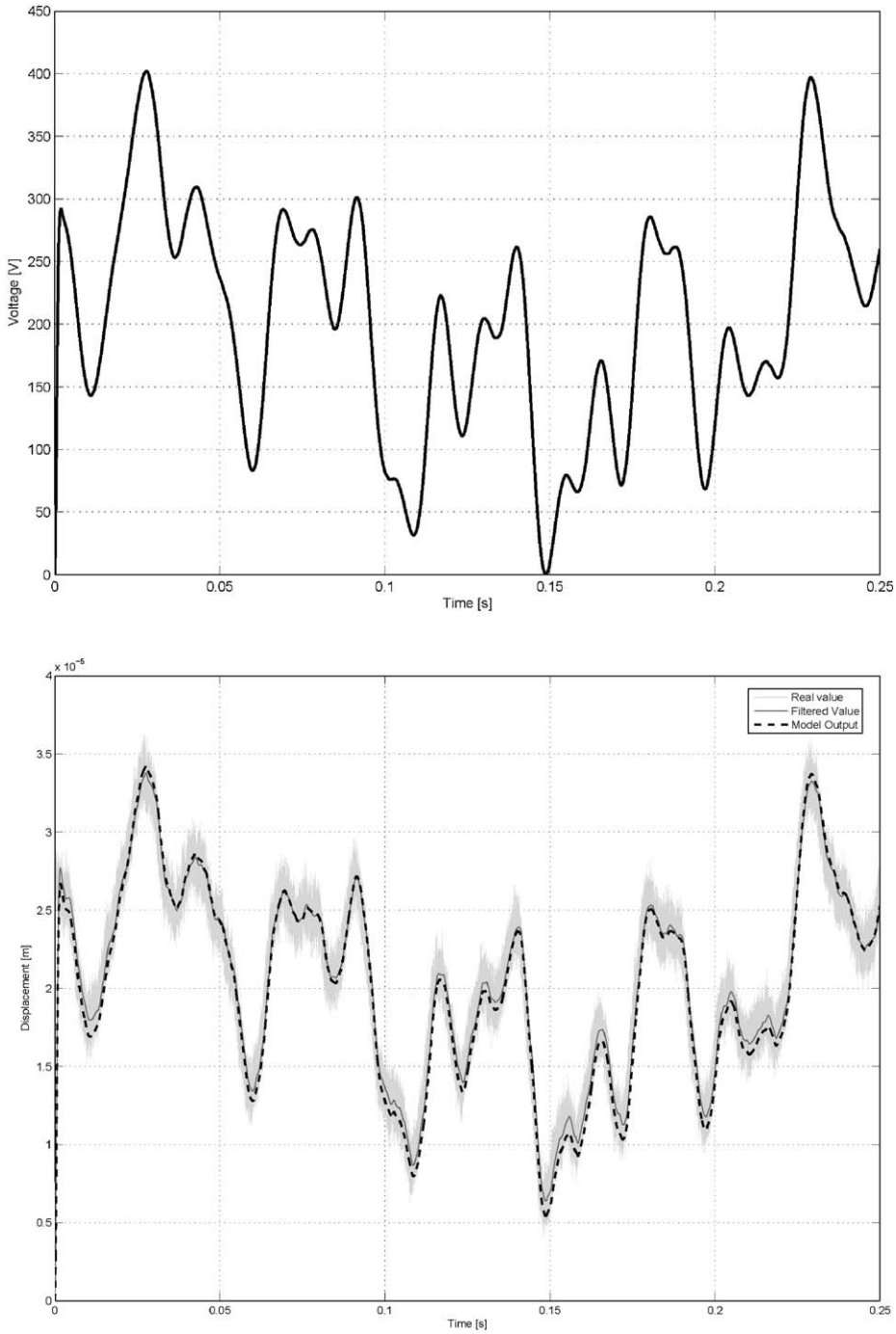

Fig. 5. Model response to a random input function.

Fig. 6 gives the behavior of the closed loop signals with $m = 5.3 \times 10^{-3}\,\mathrm{V\,s^2\,m^{-1}}$ and $c = 13\,\mathrm{V\,s\,m^{-1}}$. The initial conditions are $x_0(0) = 0\,\mathrm{m\,s}$, $x_1(0) = 20 \times 10^{-6}\,\mathrm{m}$, $x_2(0) = 0.2\,\mathrm{m\,s^{-1}}$ and $w(0) = 0$. For the reference signal, we choose y_r as the output of the second-order linear system $\omega_0^2/(s^2 + 2\xi\omega_0 s + \omega_0^2)$ with $\xi = 0.7$, $\omega_0 = 2\pi \times 500\,\mathrm{rad\,s^{-1}}$ and zero input; that is, the linear system is driven only by the nonzero initial conditions $y_r(0) = x(0)$ and $\dot{y}_r(0) = \dot{x}(0)$. It can be seen that the outputs x_1 and x_2 are regulated to zero. Note that, although the control signal $u$is zero for negative times, its asymptotic value is different from zero. This fact can be explained as follows. Taking $y_r = 0$ in Eqs. (23) and (24), it can be seen that the four states system (21)–(24) has an infinite number of equilibrium points. These equilibria are defined by $\{x_1 = 0, x_2 = 0, k_0 x_0(\infty) = \kappa_w w(\infty) = u(\infty)\}$. It is not necessary that $x_0(\infty) = 0$ so that the control value may be nonzero asymptotically (see Fig. 6). In practice, this behavior is undesirable as it implies that the actuator applies a control action at equilibrium, which means an unnecessary loss of energy. Another inconvenient of this behavior is the modification of the equilibrium point of the system.

5.2. PID plus a sinusoidal component

The previous section has pointed out to the possible modification of the equilibrium point of the system under the action of a PID controller. Since this behavior is not acceptable in practice, a modification of the controller is proposed in this section to reduce this effect. The reason for having a control which is not zero asymptotically is that $u(\infty) = \kappa_w w(\infty)$ where $w(\infty)$ is not necessarily zero. To solve this problem, the idea would be to force the hysteretic term to go to zero asymptotically, inducing the control to go to zero. Consider that system (1)–(3) is in open loop and choose for $u(t)$ a wave periodic input signal (see Section 2.2.1). Numerical simulations show that the obtained displacement signal $x(t)$ is also wave periodic. On the other hand, we know from Theorem 2 that, if the signal $x(t)$ is wave periodic, then the hysteretic output $w(\cdot)$ is also wave periodic and that it belongs asymptotically to the interval $[-\psi_{\sigma,n}(\rho(X_{\max} - X_{\min})), \psi_{\sigma,n}(\rho(X_{\max} - X_{\min}))]$. On the other hand, it can be shown that, for fixed values of the parameters σ and n, the function $\psi_{\sigma,n}(\mu)$ is increasing with its argument μ. This implies that the interval $[-\psi_{\sigma,n}(\rho(X_{\max} - X_{\min})), \psi_{\sigma,n}(\rho(X_{\max} - X_{\min}))]$ can be made as small as desired if the quantity $X_{\max} - X_{\min}$ can be reduced arbitrarily. Numerical simulations suggest that if the amplitude of the wave periodic voltage input $u(t)$ is decreased, then the amplitude of the corresponding displacement signal is also decreased.

These remarks suggest the following control law for system (1)–(3)

$$u(t) = -k_0 x_0(t) - k_1 x_1(t) - k_2 x_2(t) - A\sin(2\pi f t) \tag{25}$$

where A and f are positive design constants, and k_0, k_1, k_2 are computed using Theorem 1. The closed loop behavior is given in Figs. 7 and 8 with the values of k_0, k_1, k_2 that have been determined in the previous section, and for different values of the parameters A and f. The initial states are $x_0(0) = 0\,\mathrm{m\,s}$, $x_1(0) = 20 \times 10^{-6}\,\mathrm{m}$, $x_2(0) = 0.2\,\mathrm{m\,s^{-1}}$ and $w(0) = 0$. The reference signal is chosen as in Section 5.1.

As noticed before, the steady-state response of the closed loop is periodic, and it can be seen that the amplitude of the closed loop signals $x(t)$, $\dot{x}(t)$ and $u(t)$ decreases as A decreases. The amplitude of the steady-state closed loop signals is independent of the frequency f. This frequency influences the settling time: the transient response of the system has a shorter duration for higher frequencies f.

As a conclusion, adding a term $A\sin(2\pi f t)$ to the PID controller makes the closed loop set point oscillating around zero. The amplitude of the oscillations can be made as small as desired by reducing the design parameter A.

5.3. PID plus a sinusoidal component with a time-varying amplitude

The previous section has studied the behavior of a PID plus a sinusoidal component in the control law. It has been noticed that the set point of the closed loop steady-state systems oscillates around zero. As oscillations are also undesirable in practice, the control law has to be modified in order to eliminate them. Notice that the amplitude of the oscillations decreases with the amplitude of the sinusoidal component of the control law. This fact suggests to use for this component a time-varying amplitude that tends to decrease as the control law goes to zero. Since $u(\infty) = k_0 x_0(\infty)$ for the PID case, we choose as control law the expression:

$$u(t) = -k_0 x_0(t) - k_1 x_1(t) - k_2 x_2(t) - k_A x_0(t)\sin(2\pi f t) \tag{26}$$

where k_A is a constant gain. The system states boundedness using the proposed controller can be demonstrated by means of time-varying linear systems theory [34].

This control law has been tested using numerical simulations. The initial conditions are $x_0(0) = 0\,\mathrm{m\,s}$, $x_1(0) = 20 \times 10^{-6}\,\mathrm{m}$, $x_2(0) = 0.2\,\mathrm{m\,s^{-1}}$ and $w(0) = 0$. The reference signal is chosen as in Section 5.1.

The frequency f is taken to be 100 Hz as this value makes the settling time shorter without harming the overall response (see the previous section). Three values of k_A are chosen to study the effect of this parameter. The results of the closed loop simulations are given in Fig. 9. It can be seen that the closed loop signals x_1 and x_2 converge to zero and that larger values of k_A lead to a shorter settling time. Furthermore, the control value is the same before and after the perturbation so that the equilibrium point of the closed loop remains unchanged.

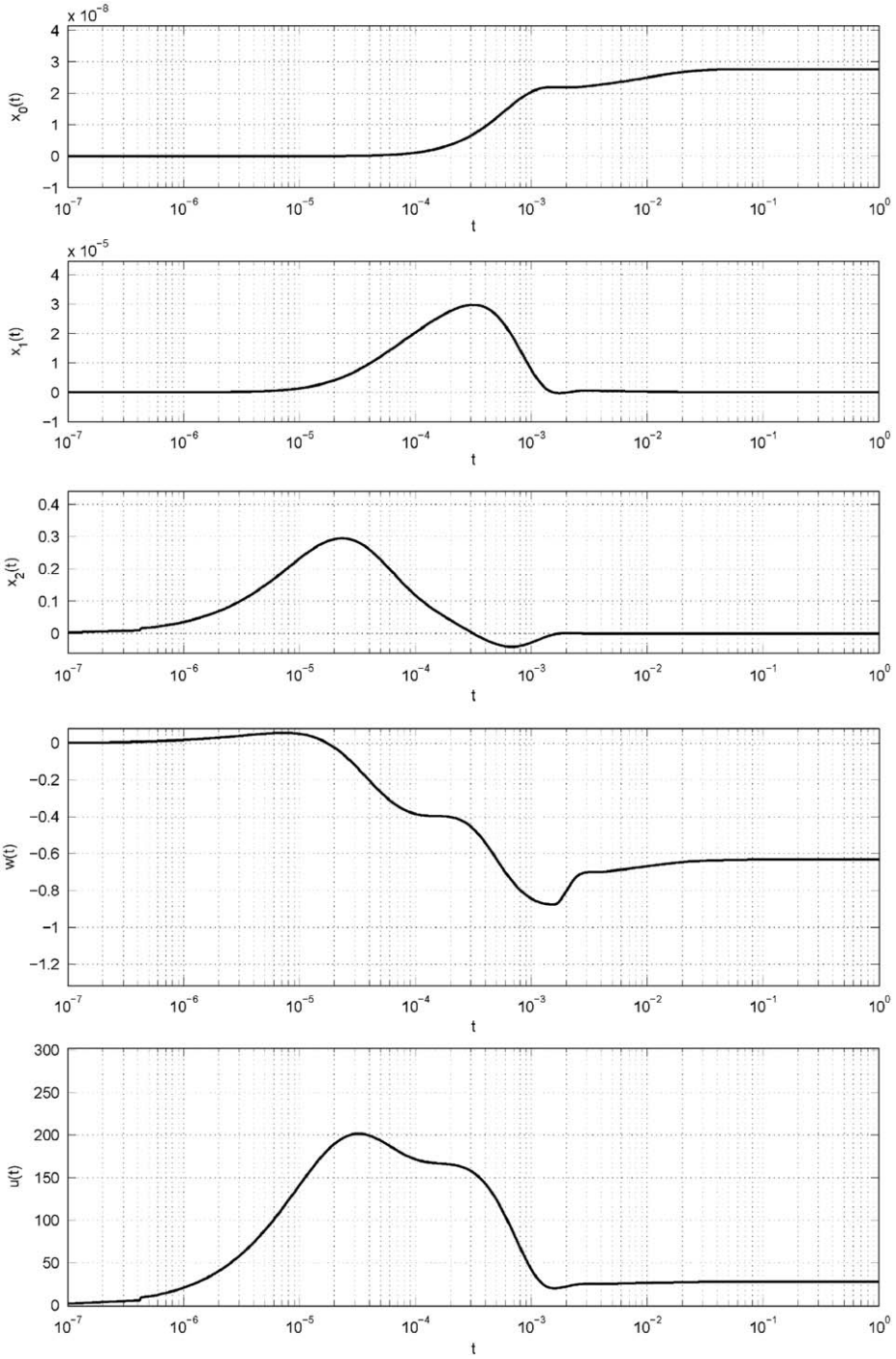

Fig. 6. Closed loop signals relative to the control law of Section 5.1.

6. Experimental results

In this section, we apply the control laws of Sections 5.1–5.3 to the piezoelectric element of Section 3.1. The numerical simulations conducted in the previous sections consisted in starting the system with nonzero initial conditions and seeing how the closed loop behaves. In our experimental platform, we first close the loop (that is we apply the control law) with a

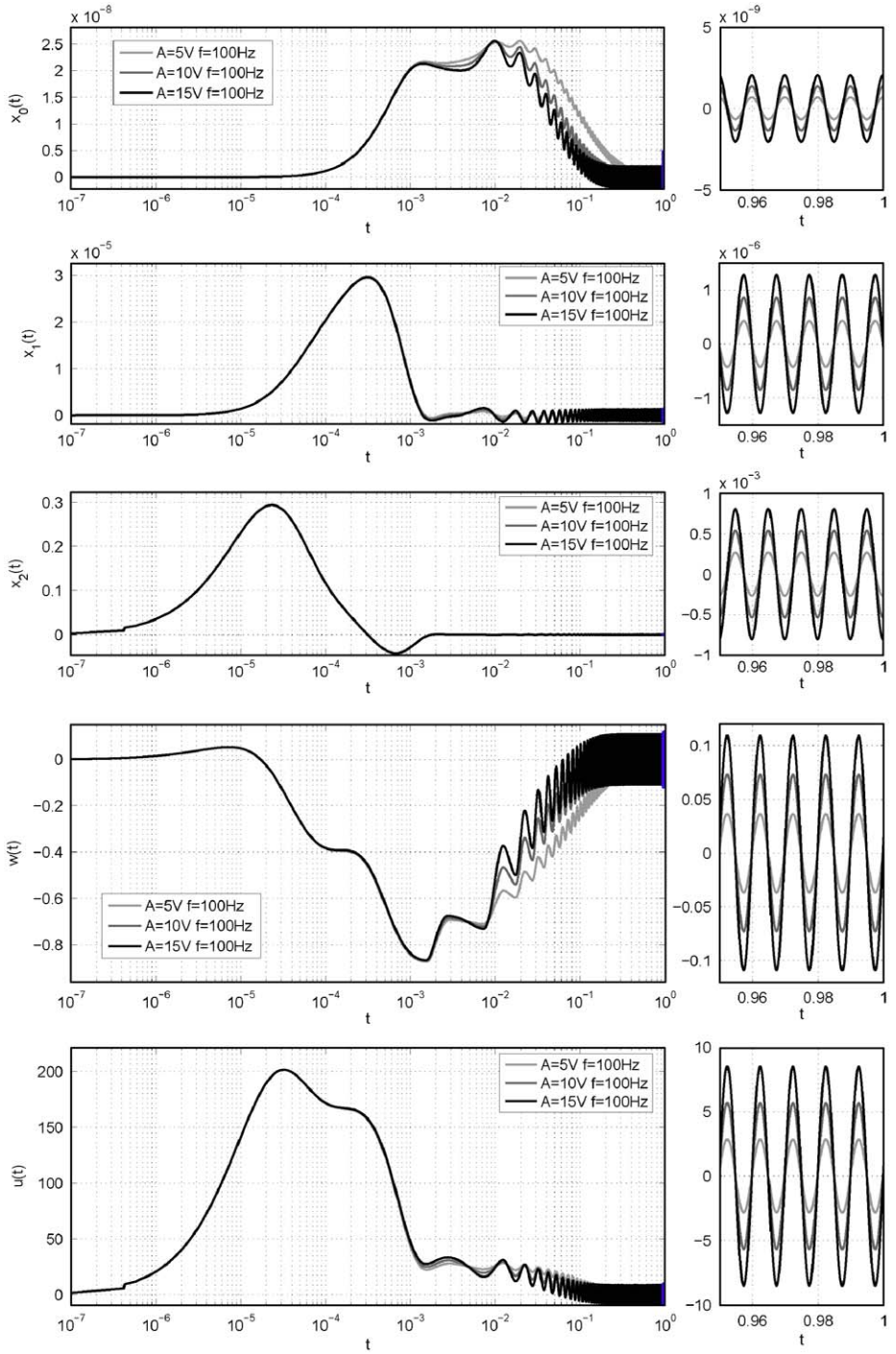

Fig. 7. Closed loop signals relative the control law of Section 5.2. The figures in the right are a zoom in the indicated region of the figures in the left.

set point for the control around 200 V. Then we open the loop during 10 ms in which the control is forced to have a constant value of 72 V. Then we closed the loop again. This time instant in which the loop is closed again corresponds to $t = 0$ in the previous numerical simulations. In this section, we take $y_r = 0$. The position of the piezoelectric element is measured directly so that the state x_1 is equal to the measured position. The state x_0 is obtained by approximating the exact integral by a sum of rectangles. The state x_2 is obtained using an Euler approximation.

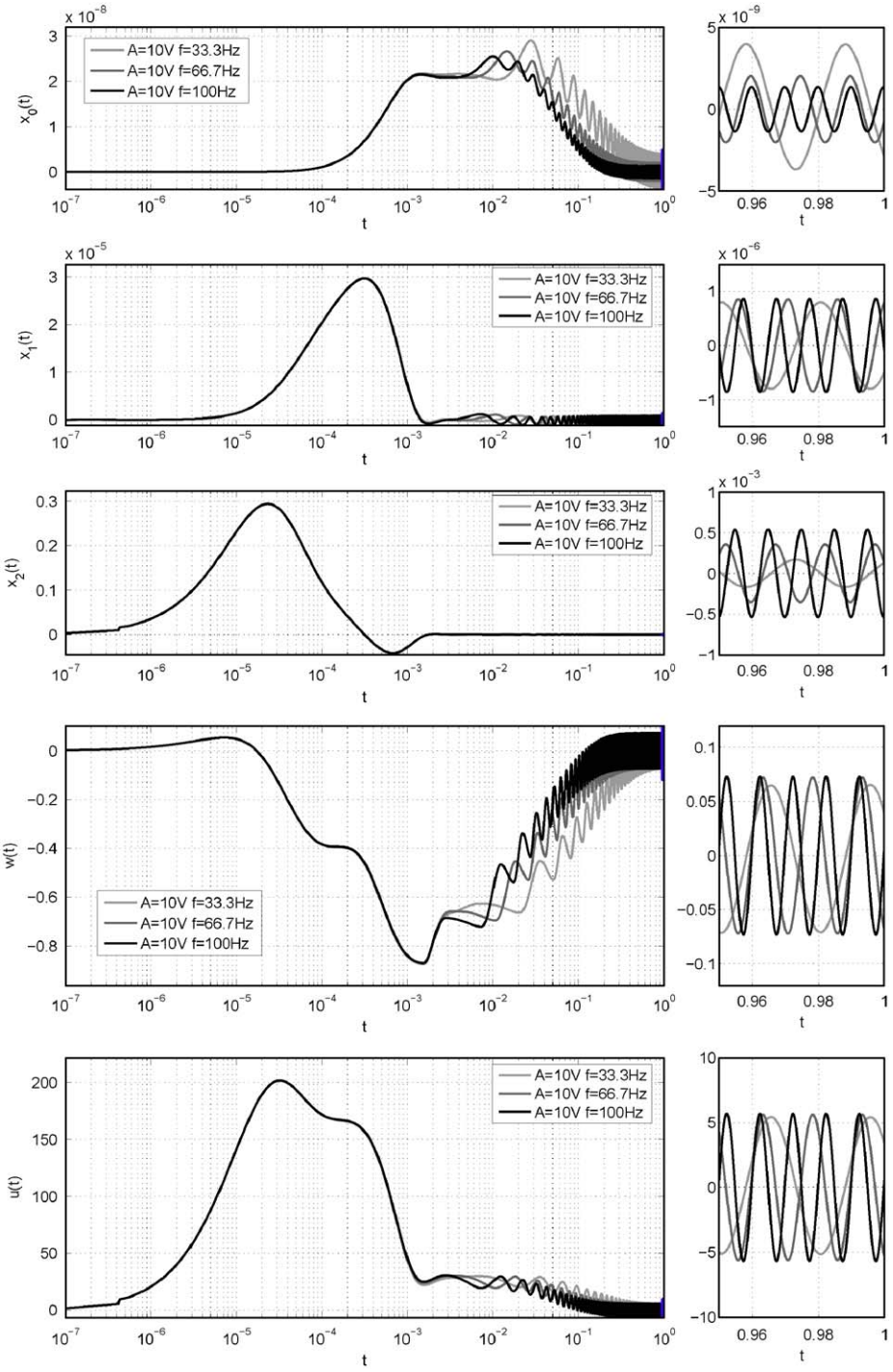

Fig. 8. Closed loop signals relative the control law of Section 5.2. The figures in the right are a zoom in the indicated region of the figures in the left.

6.1. PID control

The controller of Section 5.1 is applied to the piezoelectric element. The PID constants are the same as in Section 5.1. The closed loop signals are given in Fig. 10. As observed in the numerical simulations, the position error and the velocity go asymptotically to zero, but the final value of controller output differs from its initial value. This means that the equilibrium point of the closed loop system is not robust to perturbations.

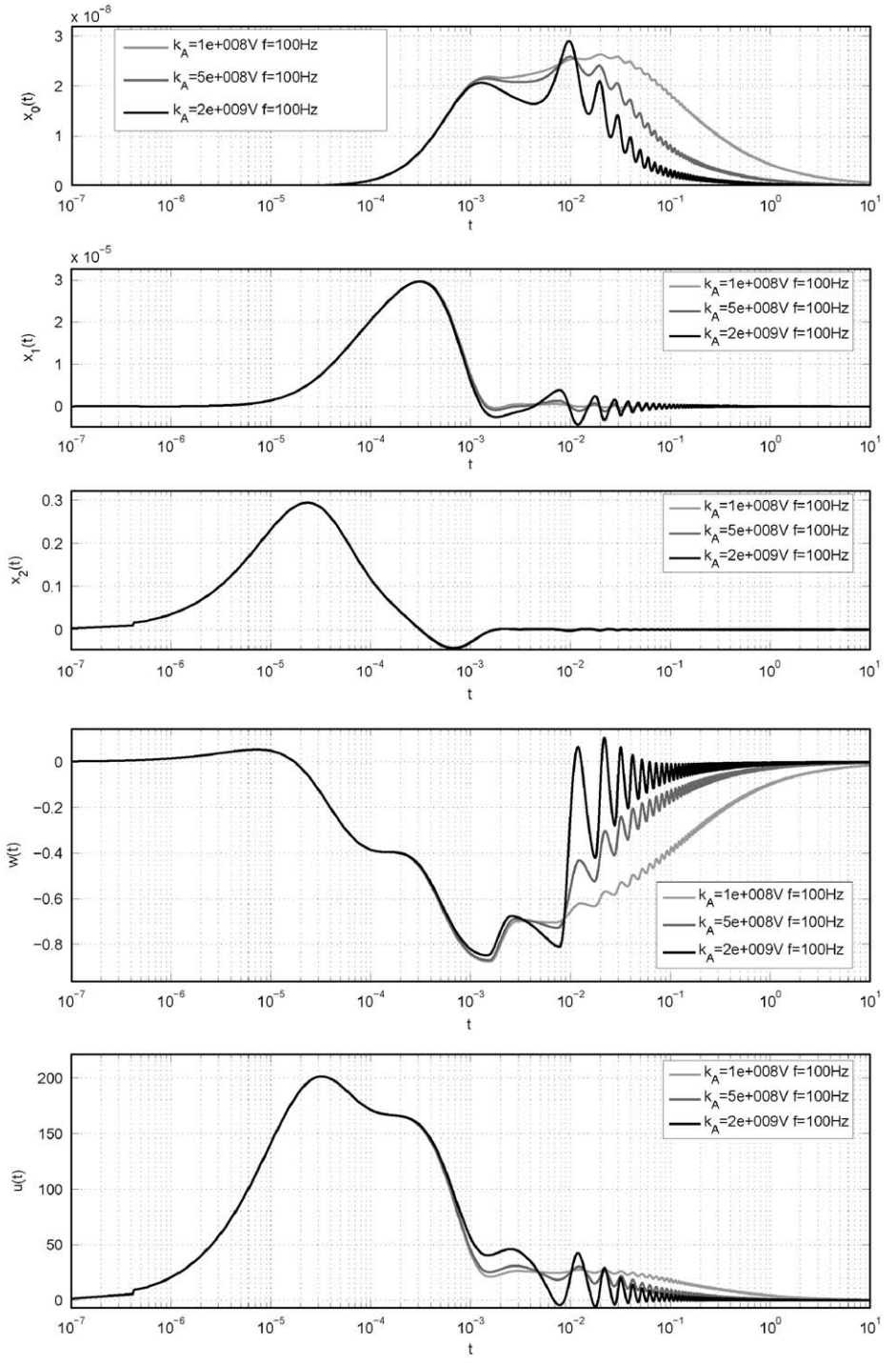

Fig. 9. Closed loop signals applying the control law introduced in Section 5.3 with $f = 100\,\text{Hz}$ and different k_A values.

6.2. PID plus a sinusoidal component

The controller of Section 5.2 is applied to the piezoelectric element. We choose $A = 15\,\text{V}$ and $f = 10\,\text{Hz}$. The constants k_0, k_1 and k_2 are the same as before. The closed loop signals are given in Fig. 11. Similar to what happens in numerical simulations, the closed loop system oscillates around zero.

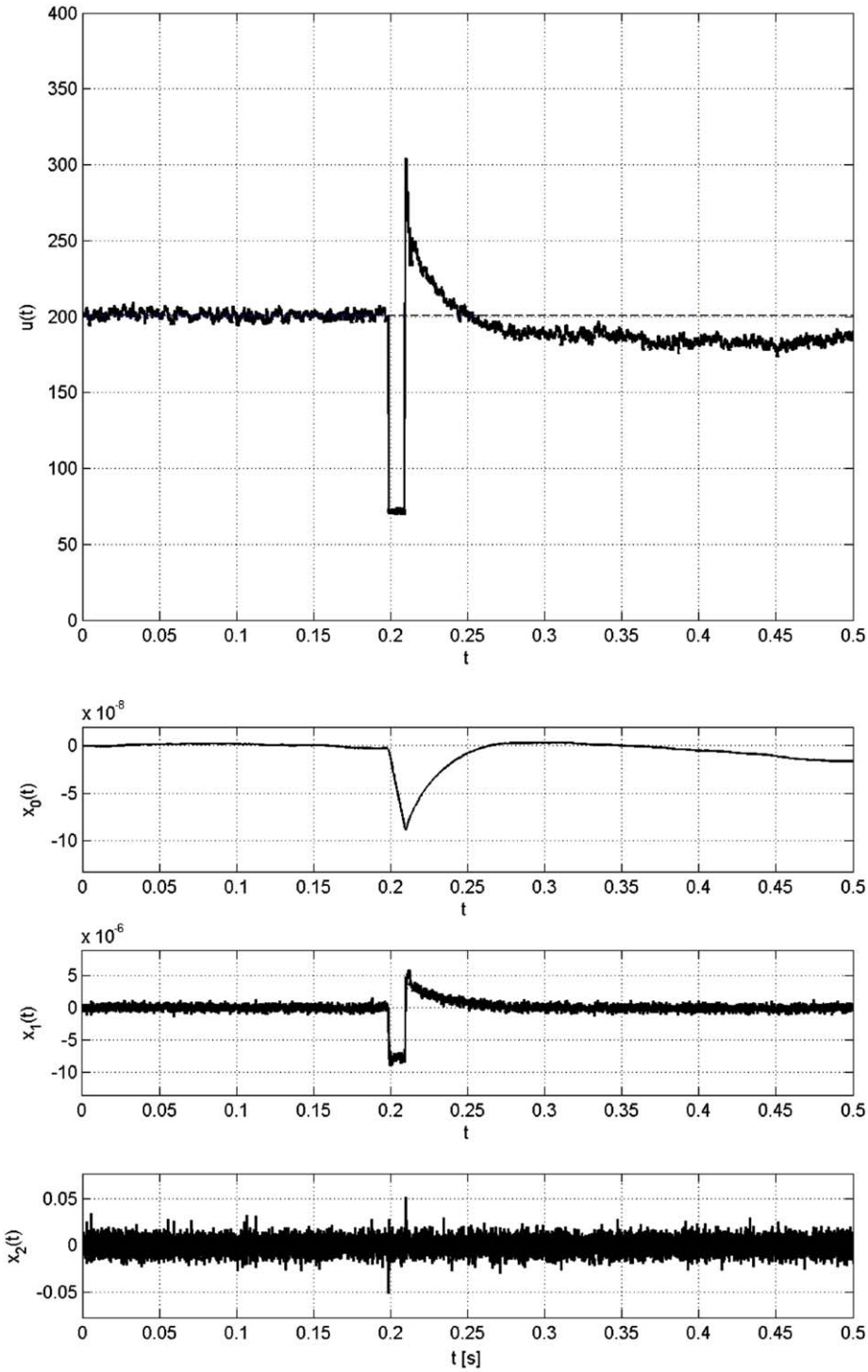

Fig. 10. Closed loop signal with the controller of Section 5.1.

6.3. PID plus a sinusoidal component with a time-varying amplitude

The controller of Section 5.3 is applied to the piezoelectric element. We choose $k_A = 1.5 \times 10^9$ and $f = 100\,\text{Hz}$. The constants k_0, k_1 and k_2 are the same as before. The closed loop signals are given in Fig. 12. It can be seen that the equilibrium point of the closed loop system is the same before and after the perturbation.

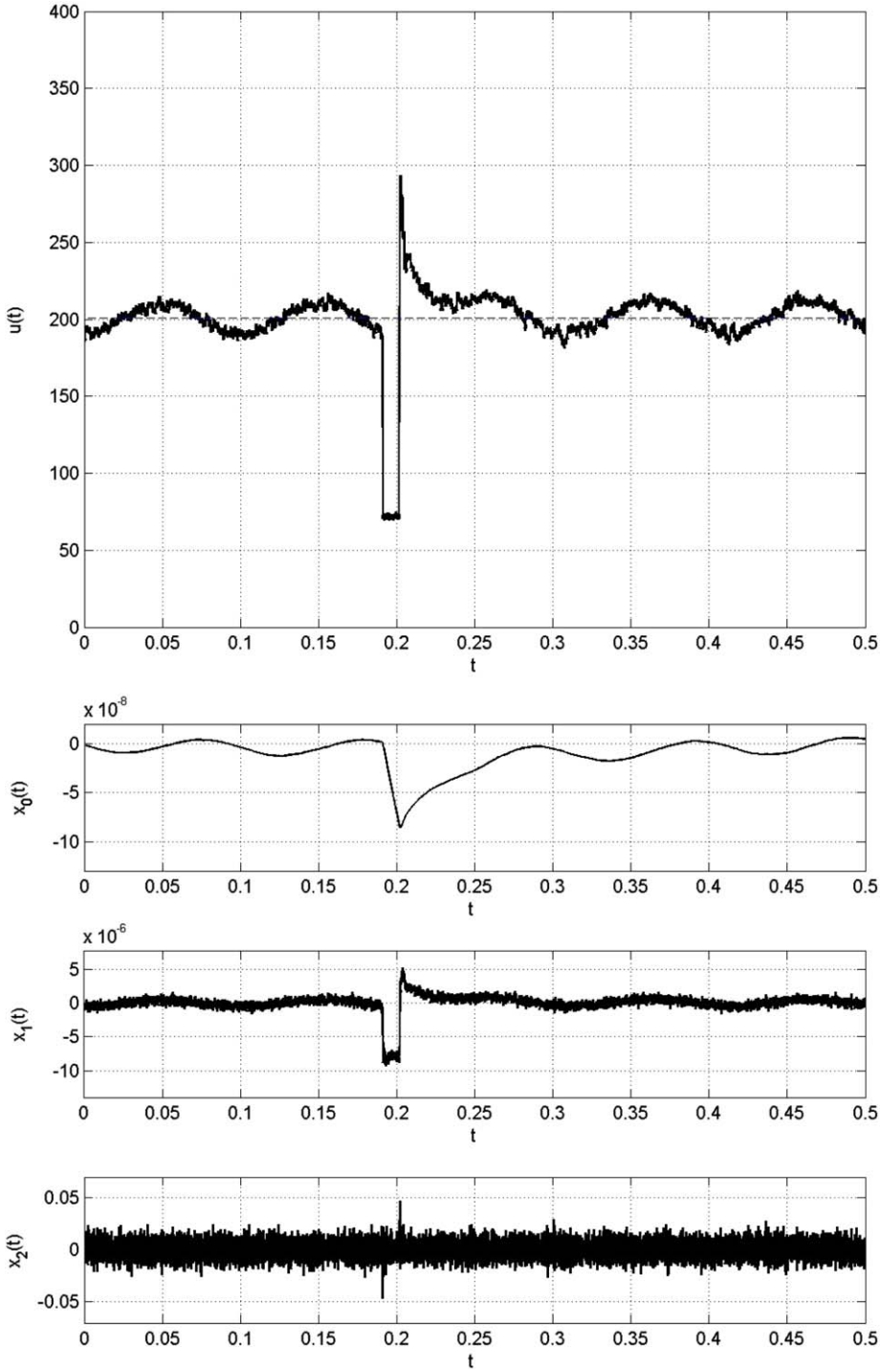

Fig. 11. Closed loop signal with the controller of Section 5.2.

7. Conclusion

This paper has presented a new control law for a piezoelectric actuator. The main challenge for the control design is the presence of hysteresis. The actuator has been represented using the Bouc–Wen model for hysteresis, and the model parameters have been identified. A nice agreement has been observed between the behavior of the piezoelectric actuator

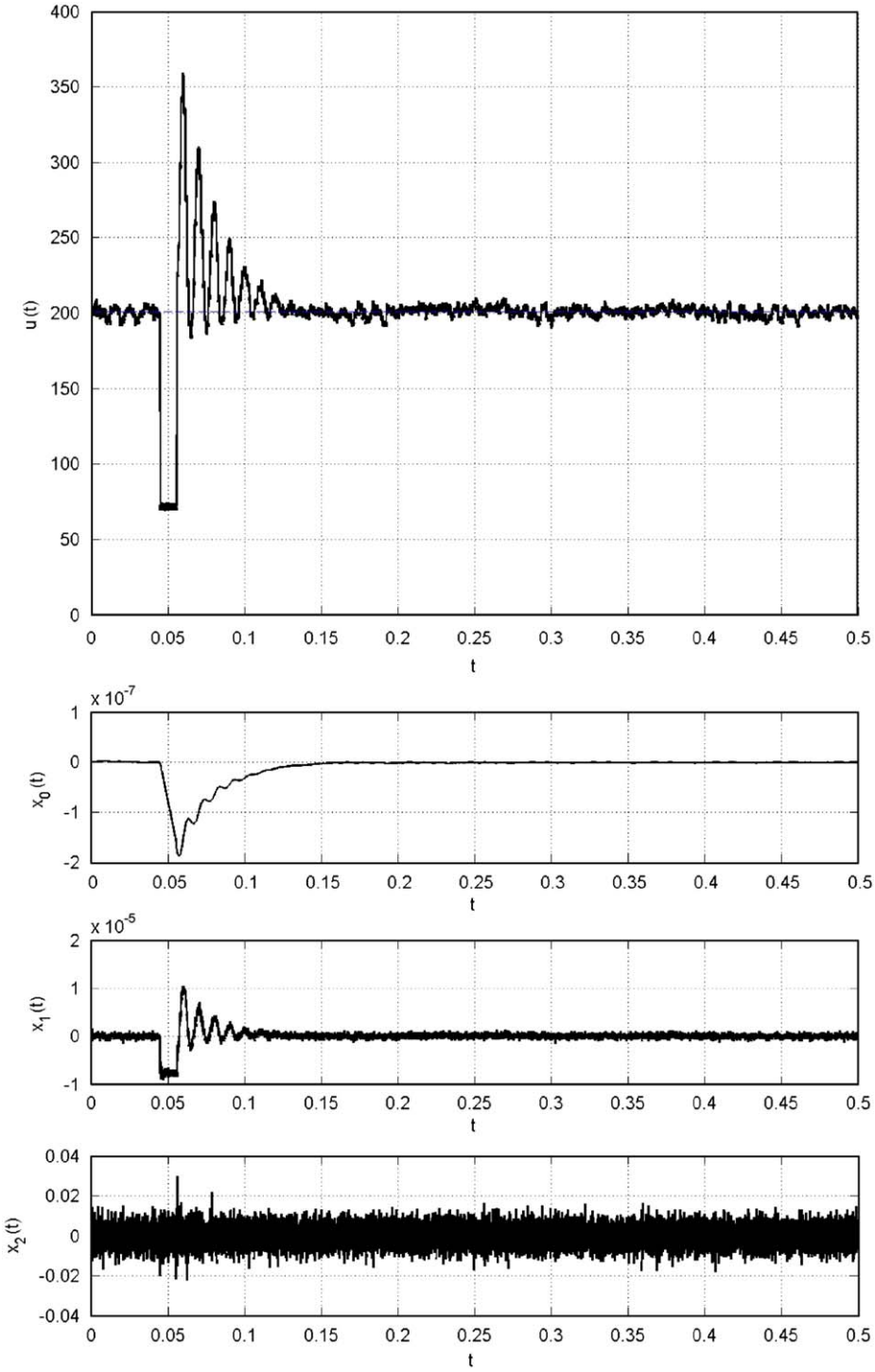

Fig. 12. Closed loop signal with the controller of Section 5.3.

and the obtained model. Then, three control laws have been tested both numerically and experimentally for the position regulation of the piezoelectric device. It has been observed that a PID with a time-varying component insures that the displacement and velocity of the actuator go to zero asymptotically, while maintaining the same equilibrium point for the closed loop system. The tracking problem for the micropositioning of the device and the developing of a model of the piezoelectric actuator for high frequencies are under investigation.

Acknowledgments

Supported by CICYT through Grants DPI2005-08668-C03-03 and DPI2005-08668-C03-01. The authors acknowledge the support of the Institute of Composite Structures and Adaptive Systems (German Aerospace Center) in Braunschweig, Germany, where the piezoelectric actuator has been assembled. The second author acknowledges the support of the Spanish Ministry of Education and Science through the "Ramón y Cajal" program.

References

[1] Y. Luo, S. Xie, X. Zhang, The actuated performance of multi layer piezoelectric actuator in active vibration control of honeycomb sandwich panel, *Journal of Sound and Vibration* 317 (2008) 496–513.
[2] M.C. Ray, A.K. Pradhan, Performance of vertically and obliquely reinforced 13 piezoelectric composites for active damping of laminated composite shells, *Journal of Sound and Vibration* 315 (2008) 816–835.
[3] V. Bhadbhade, N. Jalili, S. Nima Mahmoodi, A novel piezoelectrically actuated flexural torsional vibrating beam gyroscope, *Journal of Sound and Vibration* 311 (2008) 1305–1324.
[4] J. Curie, P. Curie, Développement par compression de l'électricité polaire dans les cristaux hémièdres à faces inclinées, *Bulletin de la Société Minéralogique de France* 3 (1880) 90–93.
[5] A. Visintin, *Differential Models of Hysteresis*, Springer, Berlin, 1994.
[6] P. Duhem, Die dauernden aenderungen und die thermodynamik, *Zeitschrift für Physikalische Chemie* 22 (1897) 543–589.
[7] M.A. Krasnosel'skii, A.M. Pokrvskii, *Systems with Hysteresis*, Nauka, Moscow, 1983.
[8] F. Preisach, Über die magnetische nachwirkung, *Zeitschrift für Physik* 94 (1935) 277–300.
[9] G.C. Foliente, Hysteresis modeling of wood joints and structural systems, *ASCE Journal of Structural Engineering* 121 (6) (1995) 1013–1022.
[10] J.W. Macki, P. Nistri, P. Zecca, Mathematical models for hysteresis, *SIAM Review* 35 (1) (1993) 94–123.
[11] C. Ru, L. Sun, Hysteresis and creep compensation for piezoelectric actuator in open-loop operation, *Sensors and Actuators A: Physical* 122 (1) (2005) 124–130.
[12] S.A. Turik, L.A. Reznitchenko, A.N. Rybjanets, S.I. Dudkina, A.V. Turik, A.A. Yesis, Preisach model and simulation of the converse piezoelectric coefficient in ferroelectric ceramics, *Journal of Applied Physics* 97 (64102) (2005) 1–4.
[13] P. Ge, M. Jouaneh, Modeling hysteresis in piezoceramic actuators, *Precision Engineering* 17 (1995) 211–221.
[14] P. Ge, M. Jouaneh, Tracking control of a piezoceramic actuator, *IEEE Transactions on Control Systems Technology* 4 (3) (1996) 209–216.
[15] Y. Pasco, A. Berry, A hybrid analytical/numerical model of hysteresis of stack actuators using a macroscopic nonlinear theory of ferroelectricity and a Preisach model of hysteresis, *Journal of Intelligent Materials, Systems and Structures* 15 (2004) 375–386.
[16] T.S. Low, W. Guo, Modeling of a three-layer piezoelectric bimorph beam with hysteresis, *Journal of Microelectromechanical Systems* 4 (4) (1995) 230–237.
[17] R.C. Smith, *Smart Material Systems: Model Development*, SIAM, Philadelphia, PA, 2005.
[18] S. Devasia, E. Eleftheriou, S.O.R. Moheimani, A survey of control issues in nanopositioning, *IEEE Transactions on Control Systems Technology* 15 (2007) 802–823.
[19] M. Goldfarb, N. Celanovic, A lumped parameter electromechanical model for describing the nonlinear behavior of piezoelectric actuators, *ASME Journal of Dynamic Systems, Measurement, and Control* 119 (1997) 478–485.
[20] S.H. Lee, M.B. Ozer, T.J. Royston, Piezoceramic hysteresis in the adaptive structural vibration control problem, *Journal of Intelligent Materials, Systems and Structures* 13 (2002) 117–124.
[21] M.B. Ozer, T.J. Royston, Passively minimizing structural sound radiation using shunted piezoelectric materials, *Journal of the Acoustical Society of America* 114 (2003) 1934–1946.
[22] Y.K. Wen, Method of random vibration of hysteretic systems, *Journal of Engineering Mechanics Division, ASCE* 102 (2) (1976) 249–263.
[23] A.W. Smyth, S.F. Masri, E.B. Kosmatopoulos, A.G. Chassiakos, T.K. Caughey, Development of adaptive modeling techniques for non-linear hysteretic systems, *International Journal of Non-Linear Mechanics* 37 (2002) 1435–1451.
[24] B.F. Spencer, S.J. Dyke, M.K. Sain, J.D. Carlson, Phenomenological model for magnetorheological dampers, *Journal of Engineering Mechanics ASCE* 123 (1997) 230–238.
[25] S.B. Choi, S.K. Lee, Y.P. Park, A hysteresis model for the field-dependent damping force of a magnetorheological damper, *Journal of Sound and Vibration* 245 (2) (2001) 375–383.
[26] B.M. Chen, T.H. Lee, C.C. Hang, Y. Guo, S. Weerasooriya, An H_∞ almost disturbance decoupling robust controller design for a piezoelectric bimorph actuator with hysteresis, *IEEE Transactions on Control Systems Technology* 7 (2) (1999) 160–174.
[27] F. Ikhouane, V. Mañosa, J. Rodellar, Adaptive control of a hysteretic structural system, *Automatica* 41 (2) (2005) 225–231.
[28] F. Ikhouane, J. Rodellar, A linear controller for hysteretic systems, *IEEE Transactions on Automatic Control* 51 (2) (2006) 340–344.
[29] V. Mañosa, F. Ikhouane, J. Rodellar, Control of uncertain non-linear systems via adaptive backstepping, *Journal of Sound and Vibration* 280 (2005) 657–680.
[30] C.-L. Hwang, C. Jan, Y.-H. Chen, Piezomechanics using intelligent variable-structure control, *IEEE Transactions on Industrial Electronics* 48 (1) (2001) 47–59.
[31] K.A. Yi, R.J. Veillette, A charge controller for linear operation of a piezoelectric stack actuator, *IEEE Transactions on Control Systems Technology* 13 (4) (2005) 517–526.
[32] F. Ikhouane, J. Rodellar, On the hysteretic Bouc–Wen model. Part I: forced limit cycle characterization, *Nonlinear Dynamics* 42 (1) (2005) 63–78.
[33] F. Ikhouane, O. Gomis-Bellmunt, A limit cycle approach for the parametric identification of hysteretic systems, *Systems & Control Letters* 57 (2008) 663–669.
[34] M. Mansour, B.D.O. Anderson, On the robust stability of time-varying linear systems, *International Series of Numerical Mathematics* 121 (1996) 135–149.